

# Journal of Materials Chemistry A

Accepted Manuscript



This is an *Accepted Manuscript*, which has been through the Royal Society of Chemistry peer review process and has been accepted for publication.

*Accepted Manuscripts* are published online shortly after acceptance, before technical editing, formatting and proof reading. Using this free service, authors can make their results available to the community, in citable form, before we publish the edited article. We will replace this *Accepted Manuscript* with the edited and formatted *Advance Article* as soon as it is available.

You can find more information about *Accepted Manuscripts* in the [Information for Authors](#).

Please note that technical editing may introduce minor changes to the text and/or graphics, which may alter content. The journal's standard [Terms & Conditions](#) and the [Ethical guidelines](#) still apply. In no event shall the Royal Society of Chemistry be held responsible for any errors or omissions in this *Accepted Manuscript* or any consequences arising from the use of any information it contains.

## Controlling Fuel Crossover and Hydration in Ultra-thin Proton Exchange Membrane based Fuel Cells using Pt-nanosheet Catalysts

Cite this: DOI: 10.1039/x0xx00000x

Rujie Wang,<sup>a,b\*\*</sup> Wenjing Zhang,<sup>a,c\*\*</sup> Gaohong He<sup>b</sup> and Ping Gao<sup>a\*</sup>

Received 00th January 2012,  
Accepted 00th January 2012

DOI: 10.1039/x0xx00000x

[www.rsc.org/](http://www.rsc.org/)

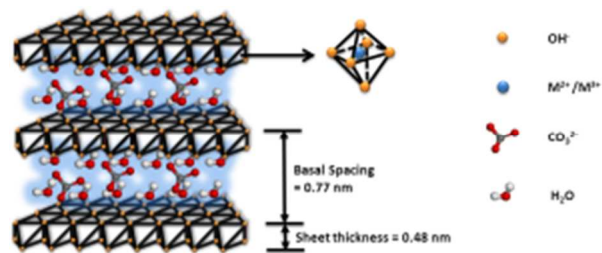
An ultra-thin proton exchange membrane with Pt-nanosheet catalysts was designed for a self-humidifying fuel cell running on H<sub>2</sub> and O<sub>2</sub>. In this design, an ultra-thin Nafion membrane was used to reduce ohmic resistance. Pt nanocatalysts were uniformly anchored on exfoliated layered double hydroxides (LDHs) nanosheets by chemical vapor deposition. After embedding Pt-LDHs nanocatalysts in 9 μm-thick Nafion membranes, exfoliated LDHs nanosheets effectively captured crossovered H<sub>2</sub> and O<sub>2</sub> through membranes. Meanwhile, Pt nanocatalysts on LDHs nanosheets catalyzed reactions between captured H<sub>2</sub> and O<sub>2</sub> and provided in-situ hydration inside Nafion membranes to maintain their proton conductivity level. Furthermore, LDHs nanosheets reinforced Nafion membranes with 181% improvement in tensile modulus and 166% improvement in yield strength. In a hydrogen fuel cell running with dry fuels, the membrane-electrode-assembly employing Pt-LDHs/Nafion membrane showed an improvement of 200% in maximum power density, an increase of 197% in current density at 0.3V and an improvement of 497% in current density at 0.5V as compared to those with Nafion 211. Pt-LDHs/Nafion membrane with a thickness of 9 μm exhibited a combination of desirable properties for the development of affordable and durable hydrogen fuel cell technology, including better mechanical properties, higher open-circuit voltage, lower ohmic resistance and enhanced water management in a hydrogen fuel cell without external humidification.

### Introduction

Fuel cells have received a significant amount of attention over the past 20 years because they have the potential for enhanced energy conversion efficiency, clean exhaust and low noise pollution<sup>1-3</sup>. From a polarization curve of fuel cell, one can clearly see that the power we can draw from a hydrogen fuel cell at a certain voltage significantly depends on ohmic resistance, which mainly arises from proton exchange membrane's (PEM's) resistance to proton conduction from anode to cathode. This has greatly sparked research interests in decreasing the resistance of PEMs without sacrificing durability and increasing cost<sup>4-7</sup>.

To reduce ohmic resistance of PEMs, two approaches have been widely explored: thinning and humidifying. On one hand, PEM's resistance to proton conduction almost linearly depends on its thickness. Therefore, over the past decade, the thickness of Nafion membranes used in hydrogen fuel cells has been progressively reduced from ~125 μm (*e.g.* Nafion 115) to 25 μm (*e.g.* Nafion 211) in order to lower ohmic sheet resistance<sup>8, 9</sup>. However, there is a limitation of thinning to extend to

considering the overwhelming fuel crossover and weak mechanical properties associated with the thinner Nafion membranes. Further reduction in membrane thickness inevitably leads to lower open-circuit voltage (OCV) and shorter PEM's life-time, which are the major concerns arisen on the practical application of 25 μm-thick Nafion membrane in hydrogen fuel cells. Therefore, extensive research efforts were made to explore the 2-dimensional (2D) nanostructured materials as fillers in PEMs to suppress the fuel crossover and improve the mechanical properties<sup>10, 11</sup>. However, common 2D fillers are too large to achieve uniform dispersion in nanoscale<sup>12</sup>. Higher dose of fillers in PEM matrix also induces reduction of proton conductivity. On the other hand, the proton conductivity of the PEM strongly increases with its water content<sup>13, 14</sup>. Therefore, in current fuel cell system, external humidifiers carrying hot water tanks are attached to fuel cell stack to constantly pump water to PEMs. Those humidifiers make fuel cell system heavier, more complicated and more expensive. Moreover, fuel cells with external humidifiers often suffer from non-uniform distribution of water in PEMs and

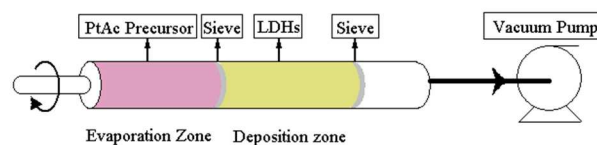


**Scheme 1.** Schematic representation of the structure of layered double hydroxides with interlayer carbonate anions.

even flooding of cathodes especially at high current density. To remove humidifiers from fuel cell system without losing power output, self-humidifying PEMs have recently emerged as an intriguing design, where nanosized Pt nanocatalysts embedded in Nafion matrix catalyze the reaction of crossover  $H_2$  and  $O_2$  to produce water for hydration of PEMs<sup>13, 14</sup>. However, the development of this design was hindered due to the agglomeration of Pt catalysts driven by the massive species migration inside the membrane and high surface energy of nanoparticles. Leaching and agglomeration of Pt catalysts lead to short circuit of fuel cells and loss of catalysts activity. Considering those critical challenges, reducing membrane thickness, lowering fuel crossover and improving Pt nanocatalysts stability is of tremendous practical importance in designing high performance self-humidifying PEMs.

In our previous work, a stable catalyst composing of Pt nanocatalysts supported by Cloisite 20A (PtOrC) was achieved by a novel design of chemical vapor deposition (CVD) synthesis protocol<sup>15</sup>. A significant self-humidification effect was clearly seen for the Pt-OrC/Nafion membrane, which delivered 170% more power output in a hydrogen fuel cell without external humidification than that of the commercial Nafion 112 membrane with similar thickness<sup>15, 16</sup>.

LDHs are a class of 2D nanostructured anionic clays. The structure of LDHs is based on brucite-like  $Mg(OH)_2$  layers, which be easily and controllably synthesized on a large scale<sup>17-24</sup>, as shown in Scheme 1. Upon calcination and reduction, metal particles can be produced that are uniformly distributed on the flakes while Mg-Al LDHs are converted into well-dispersed  $Mg(Al)O$  mixed oxides. With careful control of temperature, the platelet morphology of the calcinated LDHs (cLDHs) is usually maintained. Compared to the cationic clay used in our previous study, cLDHs have much smaller lateral size and simpler compositions, which are very important for their use in catalyst supports and barriers against fuel crossover. Herein, in this study, we used cLDHs as the substrate for Pt nanocatalysts deposition<sup>25-30</sup> and explored the idea of self-humidifying nanocomposite PEM with suppressed fuel crossover. By introducing the resulting Pt-LDHs nanocatalysts in Nafion membrane, high performance nanocomposite PEMs



**Scheme 2.** Schematic diagram of CVD reactor to synthesize nanostructured Pt catalysts on LDHs.

with thickness of 9  $\mu m$  were fabricated to show the extraordinary resistance to fuel crossover and self-humidification effects in the hydrogen fuel cells without external humidification.

## Experimental Section

### Materials

The LDHs were Mg/Al carbonate layered double hydroxides, with  $Mg^{2+}/Al^{3+}$  atomic ratio  $\sim 1.85$ , which was prepared using the coprecipitation method at 60  $^{\circ}C$  from an aqueous solution containing a mixture of  $Mg(NO_3)_2 \cdot 6H_2O$ ,  $Al(NO_3)_3 \cdot 6H_2O$ ,  $Na_2CO_3$  and NaOH at a constant pH. Cloisite 20A was provided by Southern Clay Products. Platinum (II) acetylacetonate (PtAc) was purchased from Aldrich, used as the precursor for CVD synthesis. The Nafion solution was 20 wt% polymer (equivalent weight of 1100) dissolved in low aliphatic alcohol and water, as obtained from Aldrich. DuPont de Nemours and Co. supplied the Nafion 211 membrane. Gas diffusion electrode with the Pt-loading of 0.25  $mg/cm^2$  was purchased from E-TEK. N, N-Dimethylformamide (99.5%, DMF) and N, N-dimethylacetamide (99%, DMAc) were used as co-solvents to recast the Nafion membrane. Analytical grade hydrogen and oxygen gases were used as received.

### Preparation of Pt-LDHs by direct Pt deposition on LDHs

First, Pt-deposited LDHs was synthesized by CVD method in a rotational fixed bed reactor. The CVD reactor design is described in Scheme 2. PtAc and LDHs were inserted into the evaporation zone and the deposition zone of the reactor respectively, which were separated by a powder sieve. The reaction was carried out at 350  $^{\circ}C$  for 60 minutes with a rotational speed of 90 rpm in vacuum at an absolute pressure of 23.4 mmHg. Second, to remove the organic residues, the calcination of Pt-deposited LDHs was subsequently carried out in air at 350  $^{\circ}C$  for 8 hours. Finally, hydrogen reduction of 16 hours was performed to reduce the Pt oxides using  $H_2/Ar$  gas with a volume ratio of 5:1 at a gas flow rate of 180 sccm at 350  $^{\circ}C$ . Samples will be hereafter referred to Pt-LDHs 0h and Pt-LDHs 16h. The concentration of Pt in the resulting catalysts is 1 wt% measured by XRF. For the sake of comparison, Pt-clay from direct Pt deposition on Cloisite 20A was also prepared using exactly the same CVD protocol mentioned above.

### Preparation of Pt-LDHs/Nafion nanocomposite membranes

Nanocomposite membranes were prepared via the following procedure: First, a desired amount of Pt-LDHs nanoparticles were ultrasonically mixed into ethanol. Second, 20wt% Nafion solution including DMF and DMAc was added to the mixture of Pt-LDHs and ethanol. The entire mixture was ultrasonicated using an ultrasonication probe running at pulsation mode at ambient temperature with the specific power of 20 W/g for 60 minutes. Afterwards vigorous mechanical agitation and ultrasonication at 80 °C were applied to the mixture simultaneously until the Nafion concentration in the mixture reached 20 wt%. Third, the viscous mixture was cast into a thin film using the doctor-blade technique and dried at 80 °C in a non-convection oven for 2 hours. Further drying and thermal annealing at 160 °C in vacuum for 8 hours were applied to increase the crystallinity. After thermal treatments, the membrane was washed in 0.5 M sulfuric acid at 80 °C for 1 hour twice, followed by rinsing with deionized (DI) water for several times. Finally, the membrane was stored in DI water for further use. Pt-clay/Nafion nanocomposite membrane was prepared following exactly the same procedure described above for comparison.

### Preparation of membrane electrode assembly (MEA)

First, a Nafion solution was sprayed onto the electrode to achieve a Nafion ionomer loading of 33 wt%. Then the membrane was sandwiched between 2 pieces of electrodes on both sides and uniaxially hot pressed at 135 °C and 4.0 MPa for 90 second.

### Characterization method

To investigate the crystalline structure and exfoliation nature, X-ray powder diffraction (XRD) measurements were carried out on a Philips PW 1825 diffractometer using Cu K $\alpha$  source ( $\lambda = 0.1541$  nm, 40 kV, 50 mA).

N<sub>2</sub> adsorption isotherms (Brunauer-Emmett-Teller, BET) were determined at 77 K on a Quantachrome Autosorb apparatus to study the specific surface area and pore volume.

Transmission electron microscopy (TEM) analysis was used to elucidate the Pt particle size and distribution on LDHs support on a JEOL 2010F operating at 200 kV. Pt-LDHs samples were ultrasonically dispersed in ethanol, and then deposited on a copper grid with holey carbon film for observation.

Scanning Electron Microscopy (SEM) on a JSM 6300F (JEOL) and Atomic Force Microscope (AFM) images on a Dimension 3100 were collected to examine the topography of the nanosheets deposited on silicon wafers.

To characterize the interfacial chemistry between Pt and LDHs, dynamic time-of-flight secondary ion mass spectroscopy (ToF-SIMS) was carried out on a ToF-SIMS V (Ion-ToF GmbH) spectrometer equipped with a Bi liquid metal ion gun (LMIG). Tensile properties of the membranes were measured on the Advanced Rheometrics Expansion System (ARES) at an extension rate of 2 mm/min at room temperature. Each film was

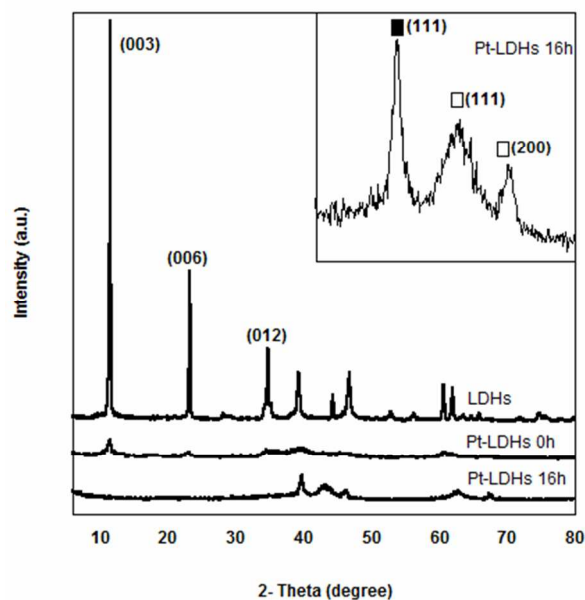


**Figure 1.** Powder XRD patterns of LDHs and Pt-LDHs nanocatalysts. Inset shows the WAXD scan of Pt-LDHs 16h in the Bragg  $2\theta$  region between 30° and 50° with labeled peaks for Pt (■) and mixed cubic MgO-like oxides (□).

cut into parallel-sided strips with dimensions of 10 × 3 mm<sup>2</sup>.

Before tensile tests, all membrane samples were predried in a vacuum oven at 105 °C for 24 hours and then cooled down to room temperature. The yield strength was obtained at 2% strain offset. Ten specimens were used for each test.

A commercial fuel cell system (FCTs, Arbin) was used to obtain the current-voltage ( $I$ - $V$ ) curves of all the MEAs using a single cell test fixture with an active geometrical area of 5 cm<sup>2</sup>. Dry H<sub>2</sub> and O<sub>2</sub> gases were fed to the cell at a minimum flow rate of 100 sccm and the backpressure of 0.1 MPa. The stoichiometric ratios were set to 1.5 for both H<sub>2</sub> and O<sub>2</sub>. The temperature of the fuel cell was controlled at 60 °C.

The limiting current associated with the H<sub>2</sub> crossover was periodically measured by linear sweep voltammetry (LSV) from 0.0 V to 0.7 V (IviumStat potentiostat). The fuel cell cathode was purged with N<sub>2</sub> at a flow rate of 200 sccm and 60 °C while H<sub>2</sub> was fed to the anode at a flow rate of 200 sccm at 60 °C.

A four point AC impedance method (IviumStat potentiostat) was used to measure the in-plane proton conductivity of membrane samples. The conductivity was calculated using Equation 1.

$$\sigma = \frac{L}{Rw\delta} \quad (1)$$

where  $L$  (cm) and  $R$  ( $\Omega$ ) are the distance and resistance between the two potential electrodes respectively,  $w$  (cm) and  $\delta$  (cm) are the width and thickness of the membranes strips.

## Results and discussion

### Preparation of stable exfoliated Pt-LDHs nanocatalysts

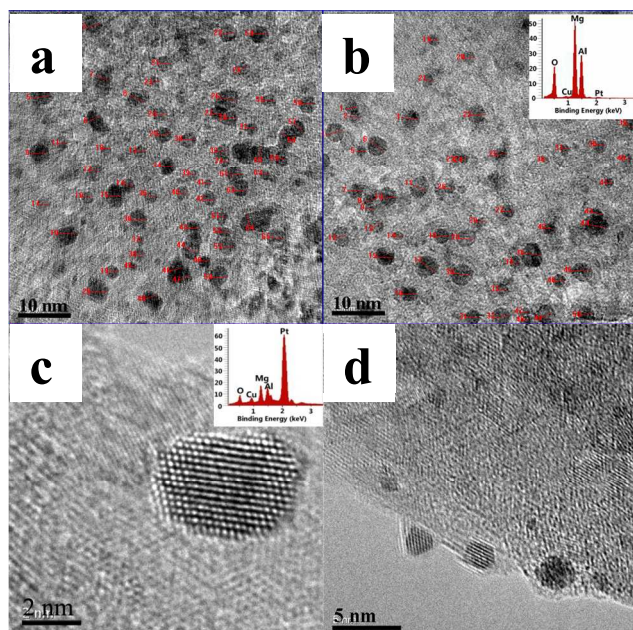


**Figure 2.** TEM images and EDS of Pt-LDHs samples. (a) Pt-LDHs 0h. (b) Pt-LDHs 16h with EDS. (c) High resolution transmission electron microscopy (HRTEM) image and EDS of the Pt particle for Pt-LDHs 16h. (d) HRTEM of Pt/LDHs interface for Pt-LDHs 16h.

The key to realizing an effective suppression of fuel crossover lies in the preparation of 2D nanostructured support with high aspect ratio where Pt nanoparticles are anchored. Herein we carefully designed the preparation protocol with the aims of: 1. the exfoliation of catalyst support, which can reduce the fuel permeability and enhance the accessibility of reactants to the Pt nanocatalysts; 2. nanostructured Pt catalysts with high crystallinity, which is essential for activity; 3. better stability of Pt nanoparticles on the support, which prevents the leaching and agglomeration of Pt nanocatalysts and ensure the long-term durability of nanocomposite PEMs.

A typical XRD pattern for the LDHs is shown in Figure 1. The sharp and symmetric features of the diffraction peaks strongly suggest the highly crystallized Mg/Al LDHs flakes stacked into a dense layered structure. However, the absence of (003) peak in the XRD spectrum of Pt-LDHs 16h nanocatalysts indicates the disappearance of the interlayered structure of LDHs. Meanwhile, (111) and (200) reflections for MgO were observed in terms of XRD spectrums, as labeled in the inset of Figure 1, revealing that crystalline periclase MgO phase was yielded during reduction step at 350 °C.

TEM images of Pt-LDHs 16h nanocatalysts are shown in Figure 2a to 2d. The corresponding EDS analyses of Figure 2b and 2c are displayed as insets respectively, identifying that the black spots on LDHs are Pt particles. As measured by image analysis software Leica Qwin, the Pt particle sizes in Pt-LDHs 0h are ranging from 1.24 to 3.89 nm, with a number-weighted mean of 2.66 nm. And the Pt particle sizes in Pt-LDHs 16h are ranging from 1.27 to 3.82 nm, with a number-weighted mean of 2.64 nm. It shows that nanostructured Pt catalysts remained

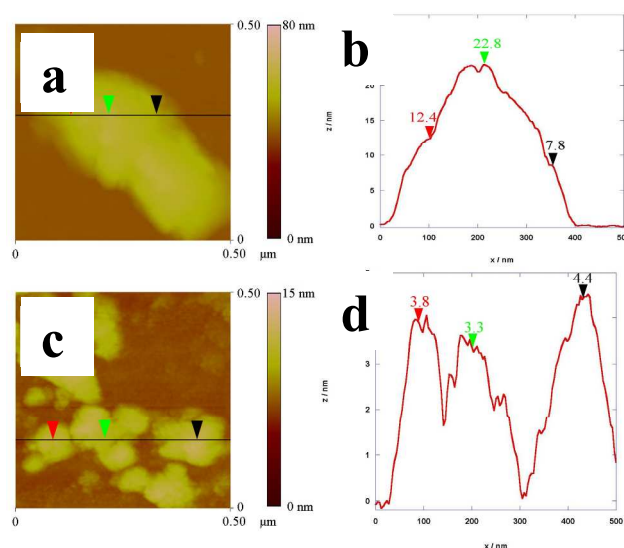


**Figure 3.** AFM images (tapping mode) of the as received LDHs and exfoliated Pt-LDHs 16h nanosheets on a Si wafer. (a) Height image of LDHs. (b) Section profile of LDHs along the marked black line in Fig. 3a. (c) Height image of Pt-LDHs 16h. (d) Section profile of Pt-LDHs 16h along the marked black line in Fig. 3c.

stable on the substrates of LDHs when the reduction was applied at 350 °C for 16 hours. Furthermore, we can deduce that the crystal plane observed here is Pt (111) facet, the thermodynamically most stable facet,<sup>25</sup> by measuring the spacing between fringes (0.226 nm from Figure 2c). Figure 2d reveals that Pt is deposited on the surface of LDHs nanosheets rather than the intralayer, which giving 430% increase in surface area (Figure S1 and Table S1 in Supporting Information), and hence improving the accessibility of the reactants to the active sites of Pt catalysts.

AFM was used to further confirm the exfoliation and visualize the morphology of Pt-LDHs nanosheets. The samples were collected by dip coating a silicon wafer in a suspension of Pt-LDHs dispersed in ethanol. Figure 3a showed the agglomeration of LDHs brucite layers with an average thickness of 15.6 nm measured by the height profile scan (as shown in Figure 3b). Very interesting, after the deposition of Pt and reduction, the sheet-like morphology of Pt-LDHs 16h nanoparticles was clearly seen in Figure 3c. The average thickness of particles is 3.3 nm. It is nearly comparable to the crystallographic thickness of monolayer Pt-LDHs nanosheets, where a single brucite layer is 0.48 nm in thickness and the Pt nanoparticle has an average size of 2 to 4 nm (by TEM). As mentioned above, the exfoliation characteristic of Pt-LDHs was revealed by XRD and BET. To the best of our knowledge, this is the first time that the morphology of exfoliated LDHs was revealed by AFM. However, it should be noted that the possibility of Pt attaching to multiple LDH sheets couldn't be excluded in this situation.

Stability of Pt catalyst plays a crucial role for the safety and cost of fuel cells. The chemical bonding in Pt-clay provides

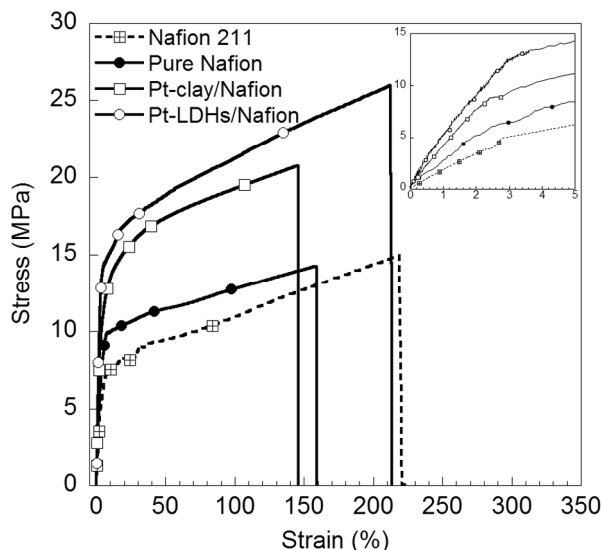


**Figure 4.** Stress–strain behavior of Nafion 211, pure Nafion, Pt-clay/Nafion and Pt-LDHs/Nafion membranes.

**Table 1.** Modulus, max strain and yield strength of Nafion 211, pure Nafion, Pt-clay/Nafion and Pt-LDHs/Nafion membranes. The tests were conducted at room temperature with the relative humidity of 40%. All membrane samples were predried in a vacuum oven at 105 °C for 24 h. Tests were performed immediately after the samples were taken out of the vacuum oven. The laboratory was conditioned at 22 °C and 40% relative humidity. The yield strength was obtained at 2% strain offset.

Samples	Modulus (MPa)	Max Strain (%)	Yield Strength (MPa)
Nafion 211	198 ± 7	219 ± 14	3.34 ± 0.21
Pure Nafion	310 ± 24	163 ± 12	5.12 ± 0.45
Pt-clay/Nafion	458 ± 38	147 ± 14	7.49 ± 0.34
Pt-LDHs/Nafion	558 ± 34	226 ± 26	8.89 ± 0.36

superior stability of Pt nanocatalysts against leaching and agglomeration as compared to weak physical attachment of Pt in conventional catalysts (*e.g.* Pt/C). Similar anchoring effect was also observed in Pt-LDHs in the present study, as shown in TEM analysis. Therefore, we carried out dynamic profiling ToF-SIMS on Pt-LDHs nanocatalysts (Figure S2 in Supporting Information). No Pt (195) or PtMgO (235) was found in as-received LDHs. However, PtMgO was observed in the spectrum of Pt-LDHs samples. It suggests that the chemical bond, Pt-O-Mg as recommended, was established between Pt and LDHs during the CVD synthesis.

#### Mechanical properties of ultrathin Pt-LDHs/Nafion nanocomposite membranes

With the confidence in the activity and stability of Pt-LDHs 16h, we furthered our study by uniformly dispersing Pt-LDHs 16h nanocatalysts in the Nafion membrane.

Vehicles, portable devices, and remote or on-site installations employing fuel cells must tolerate frequent startup, shutdown and power load cycles. Surviving these cycles will require the development of cost-effective, high-performance, advanced PEM materials<sup>26, 27</sup>. Industrial production of ultra-thin membrane for MEAs poses the challenges of roll-to-roll continuous production of materials with weak mechanical properties. Thus, mechanical properties such as tensile modulus, yield strength and max strain should be taken into account to develop the ultrathin membranes in this study.

Figure 4 and Table 1 show the tensile tests results of commercial Nafion 211, pure Nafion, Pt-clay/Nafion and Pt-LDHs/Nafion membranes. Utilizing Pt-LDHs 16h nanocatalysts as reinforcement, Pt-LDHs/Nafion exhibited 181% improvement in modulus and 166% improvement in yield strength as compared to Nafion 211. Moreover, the advantages of using Pt-LDHs 16h as the nanofillers are clearly seen as compared to Pt-clay due to the relatively small particle size and better dispersion of Pt-LDHs in Nafion matrix.

It should be noted that, the ultra-thin Pt-LDHs/Nafion membrane, having the thickness of ~ 9 μm, is able to tolerate the same amount of tensile stress as Nafion membrane of 25.4 μm (9 μm \* 558 MPa / 198 MPa = 25.4 μm), while Nafion membrane of 25 μm is the most used PEM in the current fuel cell systems. Therefore, the ultrathin Nafion membranes (~9 μm in thickness) bearing Pt-LDHs or Pt-clay nanocatalysts were prepared and tested as the PEMs in hydrogen fuel cells. Based on the tests on the Pt-LDHs nanocatalysts, Pt-LDHs 16h with high Pt activity, strong stability and high surface area is highly desirable as the nanofiller for the preparation of self-humidifying PEMs. As shown in Table 2, the catalyst concentration in Pt-clay/Nafion or Pt-LDHs/Nafion is 1 wt% based on the total weight of the composite membrane. The thickness of the resulting membranes is around 9 μm. For the sake of comparison, pure Nafion (cast from 20 wt% Nafion dispersion) and commercial Nafion 211 were tested as PEMs in fuel cells.

**Table 2.** Thickness and composition of PEMs used in this study.

Membranes	Catalyst Concentration (% w/w)	Thickness (μm)
Nafion 211	0	25.0
Pure Nafion	0	8.9
Pt-clay/Nafion	1 (Pt-clay)	9.0
Pt-LDHs/Nafion	1 (Pt-LDHs 16h)	8.9

#### Proton conductivity of the PEMs

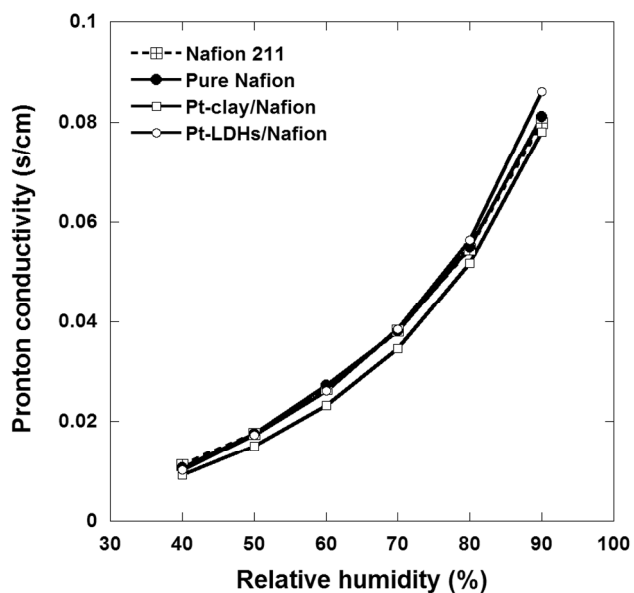


**Figure 5.** Proton conductivity of Nafion 211, pure Nafion, Pt-clay/Nafion and Pt-LDHs/Nafion membranes with different humidity at 60 °C. All membranes were cut into parallel-sided strips with dimensions of 10 x 3 mm<sup>2</sup> and were boiled in 0.5 M H<sub>2</sub>SO<sub>4</sub> solution for 1 h and in DI water for 1 h. Proton conductivity was measured in a humidity chamber at 60 °C and varied relative humidity.

The proton conductivity of membranes was measured by a four point AC impedance method in a chamber with humidity control. The similar and slightly higher proton conductivity of Pt-LDHs/Nafion and Pt-clay/Nafion were observed as compared to pure Nafion and Nafion 211 in the full range of relative humidity in Figure 5.

Therefore the incorporation of Pt-clay and Pt-LDHs in the composite membranes didn't decrease the mobility of hydronium ions across the membrane. The similarity in proton conductivity was further proved in the fuel cell tests, where the slopes of polarization curves for the MEAs with pure Nafion, Pt-clay/Nafion and Pt-LDHs/Nafion were the same.

#### Performance of ultra-thin Pt-LDHs/Nafion PEMs in hydrogen fuel cell

During the operation of hydrogen fuel cells, dry H<sub>2</sub> and O<sub>2</sub> gases were fed to the cell with a flow rate of 100 sccm under the backpressure of 0.1 MPa at 60 °C. The polarization curves were shown in Figure 6. It should be noticed that the low open circuit voltage (OCV) is not uncommon for the fuel cell running with dry gases and ultrathin PEMs due to the severe gas crossover through the membrane. In addition, the relatively low Pt loading on the cathode (0.25 mg<sub>Pt</sub>/cm<sup>2</sup>) decreased the exchange current density on electrodes and therefore induced the larger activation overpotential.

Under the same operation conditions, however, the difference in OCV is believed to be caused only by the amount of fuel crossover through PEMs. As shown in Table 3, the MEA with

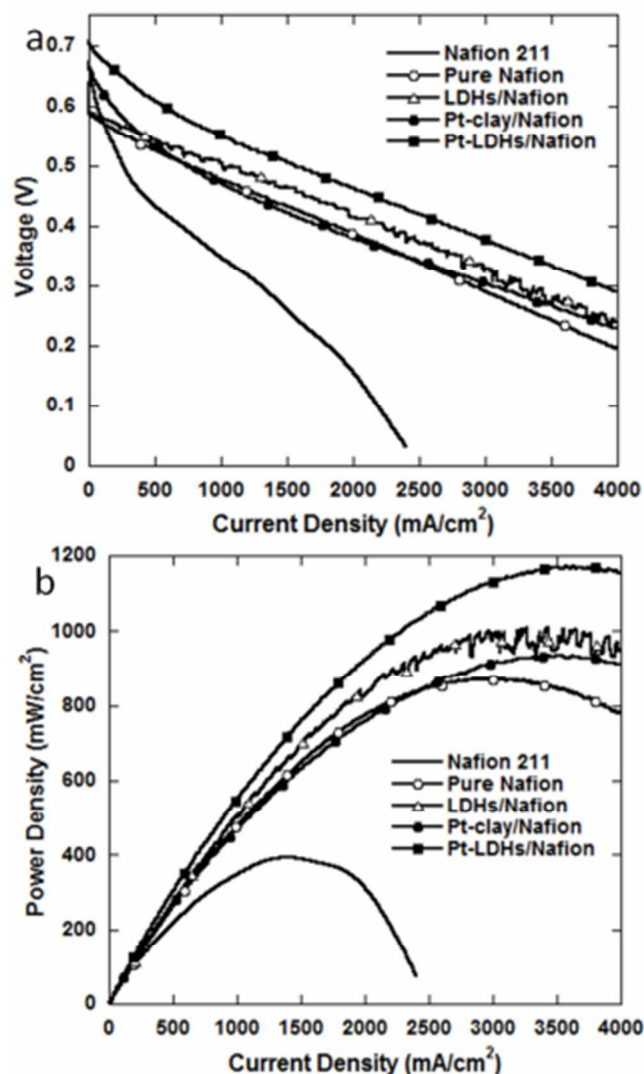


**Figure 6.** Polarization curves of the hydrogen fuel cells employing MEAs with Nafion 211 (25 μm), pure Nafion (8.9 μm), LDHs/Nafion (9 μm), Pt-clay/Nafion (9 μm) and Pt-LDHs/Nafion (8.9 μm) membranes. The stoichiometric ratios were set to 1.5 for H<sub>2</sub> and O<sub>2</sub> and the minimum flow rates of H<sub>2</sub> and O<sub>2</sub> were 100 sccm without external humidification. The fuel cell was operated at 60 °C under a back pressure of 0.1 MPa.

pure Nafion membrane with the thickness of 9 μm exhibited an OCV of 0.587V, which is considerably lower than the OCV given by Nafion 211 (25 μm) due to the difference in thickness. With the presence of Pt-LDHs or Pt-clay, there was an increase in OCVs for MEAs employing the composite PEM (0.666V for Pt-clay/Nafion and 0.705V for Pt-LDHs/Nafion). With the same amount of nanocatalysts (1wt% based on the total weight of composite membrane), Pt-LDHs had a better dispersion in Nafion matrix than Pt-clay, which contributed to the better fuel crossover barrier and therefore higher OCV as compared to the MEA with Pt-clay/Nafion. To quantify the fuel crossover in a

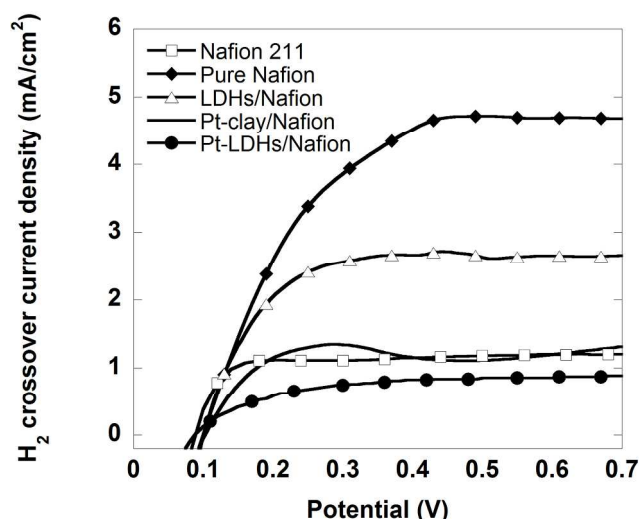


**Figure 7.** Linear sweep voltammograms (LSV) for hydrogen crossover on the MEAs of Nafion 211 (25  $\mu\text{m}$ ), pure Nafion (8.9  $\mu\text{m}$ ), LDHs/Nafion (9  $\mu\text{m}$ ), Pt-clay/Nafion (9  $\mu\text{m}$ ) and Pt-LDHs/Nafion (8.9  $\mu\text{m}$ ) membranes. The limiting current density associated with the hydrogen crossover was measured by LSV from 0.0 V to 0.7 V. The fuel cell cathode was purged with  $\text{N}_2$  at a flow rate of 200 sccm and 60  $^\circ\text{C}$  while  $\text{H}_2$  was fed to the anode at a flow rate of 200 sccm at 60  $^\circ\text{C}$ .

**Table 3.** OCV, the maximum power density and the current density at 0.5V and 0.3V of the MEAs with Nafion 211, pure Nafion, LDHs/Nafion, Pt-clay/Nafion and Pt-LDHs/Nafion membranes tested in a single hydrogen fuel cell.

MEAs	Nafion 211	Pure Nafion	LDHs/Nafion	Pt-clay/Nafion	Pt-LDHs/Nafion
OCV	0.671	0.587	0.638	0.666	0.705
Maximum Power density ( $\text{mW}/\text{cm}^2$ )	391	873	1007	936	1174
Current Density at 0.5V ( $\text{mA}/\text{cm}^2$ )	261	754	1012	743	1558
Current Density at 0.3V ( $\text{mA}/\text{cm}^2$ )	1301	2897	3271	3036	3863

running fuel cell, *in-situ* linear sweep voltammetry (LSV) was used for all MEAs to monitor the limiting current density on the cathode side where the  $\text{O}_2$  was replaced by dry  $\text{N}_2$ . The higher limiting current density in Figure 7 indicated the higher fuel crossover through the PEMs. Consistent with the difference in OCVs, a dramatic reduction in fuel crossover for the membrane bearing Pt-LDHs or Pt-clay was clearly seen in Figure 7. Especially for the MEA with Pt-LDHs/Nafion, the limiting current is only  $\sim 0.85 \text{ mA}/\text{cm}^2$ . It represents 82% reduction in fuel crossover as compared to pure Nafion with the same thickness. It should be emphasized that Pt-LDHs/Nafion membrane, with 64% reduction in thickness, exhibited an OCV higher than that of commercial Nafion 211. It proves that the

severe hydrogen crossover, as the major challenge in the practical application of ultrathin membranes in hydrogen fuel cells, can be overcome by uniformly embedding stable Pt-LDHs nanocatalysts in Nafion matrix.

In the low current density region, the MEA of Pt-clay/Nafion showed a higher activation overpotential than that of Pt-LDHs/Nafion and pure Nafion. The completion of the overall reaction in hydrogen fuel cells requires the simultaneous deliveries of  $\text{O}_2$  from gas diffusion layer, electrons from the anode (through external circuit) and the protons from the membrane to the active sites of Pt catalysts. It is hypothesized that the presence of Pt-clay on the interface of the membrane and the cathode may interfere with the proton transfer from the membrane to the active sites of Pt in cathode. The adverse influence was apparently suppressed by the smaller size and better dispersion of Pt-LDHs in Nafion. Moreover, a remarkable improvement in performance at high current density region was clearly seen for all the MEAs with ultrathin membranes. Due to the current capacity of the fuel cell test station, the maximum current density we were able to obtain for  $5 \text{ cm}^2$  MEA was  $4000 \text{ mA}/\text{cm}^2$ . For the MEA with 25  $\mu\text{m}$ -thick Nafion 211 membranes, an abrupt drop in voltage (severe anode drying) was observed when the current density was over  $1000 \text{ mA}/\text{cm}^2$ , resulted from the huge electro-osmotic drag of water from the anode to the cathode. It is particularly interesting that no limiting current was observed for all the MEAs employing ultrathin membranes (pure Nafion, Pt-clay/Nafion and Pt-LDHs/Nafion) till the current density reached  $4000 \text{ mA}/\text{cm}^2$ . Therefore, the use of the ultrathin membranes in hydrogen fuel cells may contribute to a better water management and even the delay of severe anode drying at high current density region.

Benefiting from the significant suppression of fuel crossover by the use of Pt-LDHs nanocatalysts and the enhanced water management by the use of ultrathin membrane, the polarization curve of MEA with Pt-LDHs/Nafion was well above the voltage of the MEA with Nafion 211 in the full range of current density. As shown in Table 3, the MEA with Pt-LDHs/Nafion delivered a maximum power density of  $1174 \text{ mW}/\text{cm}^2$  and a current density of  $1558 \text{ mA}/\text{cm}^2$  at 0.5V, which represent an improvement of 200% and 497% respectively as compared to the MEA with Nafion 211.

Though the crossover has been dramatically suppressed by the incorporation of Pt-LDHs, the crossover and stability remain the major concerns for such ultra-thin membranes. Life-test should be conducted before applications.

## Conclusions

A significant suppression of fuel crossover in an ultrathin Nafion membrane was achieved by the incorporation of the exfoliated Pt-LDHs nanocatalysts. First, a CVD synthesis protocol followed by thermal treatment and reduction was carefully designed and optimized to develop a stable Pt nanocatalyst supported by exfoliated LDHs nanosheets. In XRD results, the absence of the (0 0 3) diffraction peaks for

interlayer gallery structure proved the exfoliation of LDHs of Pt nanoparticles by CVD. Under TEM, Pt nanoparticles with an average diameter of 2 to 4 nm were found to be uniformly distributed on the exfoliated LDHs nanosheets. The monolayer deposition of Pt nanocatalysts on the single LDHs nanosheet was revealed by AFM analysis. Therefore, a significant increase in BET surface area was observed for Pt-LDHs as compared to as-received LDHs. By ToF-SIMS, Pt nanoparticles were found chemically bonded to LDHs nanosheets. Pt-LDHs 16h exhibited the highest BET surface area and strong chemical bonding between Pt nanoparticles and exfoliated LDHs nanosheets, where the highly crystallized Pt catalysts have an average diameter of 2.64 nm.

Secondly, a nanocomposite Nafion membrane employing 1wt% Pt-LDHs 16h was prepared and tested as the PEM in a hydrogen fuel cell. In LSV tests, a tremendous reduction in fuel crossover was observed in Pt-LDHs/Nafion membrane as compared to pure Nafion with the same thickness (9  $\mu\text{m}$ ), which resulted in an OCV higher than that of Nafion 211 (25  $\mu\text{m}$ ) in a hydrogen fuel cell test. Meanwhile, the better dispersion of Pt-LDHs not only significantly suppressed the fuel crossover but also reduced the adverse influence on proton transport from the membrane to the catalyst layer as compared to Pt-clay. Therefore a higher OCV and lower activation overpotential were seen in the MEA with Pt-LDHs/Nafion than that of Pt-clay/Nafion. Moreover, the performance of the MEA was further enhanced by the use of ultrathin membranes, which showed a significant improvement in water management and even the delay of severe anode drying at high current density region. In a hydrogen fuel cell running with dry fuels at 60  $^{\circ}\text{C}$ , the MEA employing Pt-LDHs/Nafion membrane delivered a maximum power density of 1174  $\text{mW}/\text{cm}^2$  and a current density of 1558  $\text{mA}/\text{cm}^2$  at 0.5V, which represents improvements of 200% and 497% respectively as compared to the MEA with Nafion 211. The synergetic effects of self-humidification and fuel crossover suppression by using exfoliated Pt-LDHs nanocatalyst in Nafion membrane presented a promising PEM candidate for the affordable and durable hydrogen fuel cell technology.

## Acknowledgements

Rujie Wang and Wenjing Zhang contributed equally. The project was sponsored by the Research Grant Council of Hong Kong with an earmarked grant for research (612805).

## Notes and references

<sup>a</sup> Department of Chemical and Biomolecular Engineering, Hong Kong University of Science and Technology, Clear Water Bay, Kowloon, Hong Kong SAR, People's Republic of China. E-mail: kepgao@ust.hk

<sup>b</sup> The R&D Center of Membrane Science and Technology, Dalian University of Technology, 2 Linggong Road, Dalian, People's Republic of China.

<sup>c</sup> Department of Energy Conversion and Storage, Technical University of Denmark, DK-4000 Roskilde, Denmark

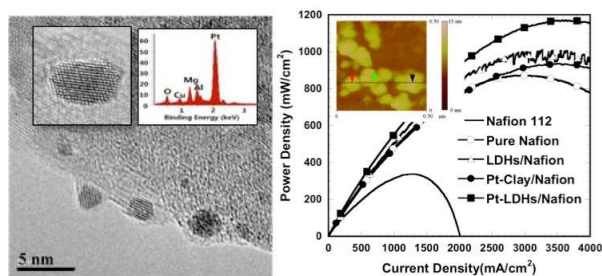
Electronic Supplementary Information (ESI) available: [details of any supplementary information available should be included here]. See DOI: 10.1039/b000000x/

1. V. S. Murthi, J. Dura, S. Satija and C. Majkrzak, *ECS Trans.*, 2008, **16**, 1471-1485.
2. X. Xie, S. Chen, W. Ding, Y. Nie and Z. Wei, *Chem. Commun.*, 2013, **49**, 10112-10114.
3. J. A. Mader and B. C. Benicewicz, *Macromolecules*, 2010, **43**, 6706-6715.
4. A. A. Kornyshev, A. M. Kuznetsov, E. Spohr and J. Ulstrup, *J. Phys. Chem. B*, 2003, **107**, 3351-3366.
5. M. Eikerling, A. A. Kornyshev, A. M. Kuznetsov, J. Ulstrup and S. Walbran, *J. Phys. Chem. B*, 2001, **105**, 3646-3662.
6. H. N. Yang, D. C. Lee, S. H. Park and W. J. Kim, *J. Membr. Sci.*, 2013, **443**, 210-218.
7. L. Du, X. Yan, G. He, X. Wu, Z. Hu and Y. Wang, *Int. J. Hydrogen Energy*, 2012, **37**, 11853-11861.
8. T. E. Springer, T. A. Zawodzinski and S. Gottesfeld, *J. Electrochem. Soc.*, 1991, **138**, 2334-2342.
9. K. Prater, *J. Power Sources*, 1990, **29**, 239-250.
10. C. C. Yang and Y. J. Lee, *Thin Solid Films*, 2009, **517**, 4735-4740.
11. P. Bebin, M. Caravanier and H. Galiano, *J. Membr. Sci.*, 2006, **278**, 35-42.
12. C. Hung-Chung, T. Li-Duan, L. Chien-Ming, L. Jiunn-Nan, Z. Chao-Yuan and C. Feng-Chih, *J. Power Sources*, 2013, **226**, 87-93.
13. M. Watanabe, H. Uchida, Y. Seki, M. Emori and P. Stonehart, *J. Electrochem. Soc.*, 1996, **143**, 3847-3852.
14. H. Hagihara, H. Uchida and M. Watanabe, *Electrochim. Acta*, 2006, **51**, 3979-3985.
15. W. J. Zhang, M. K. S. Li, R. J. Wang, P. L. Yue and P. Gao, *Langmuir*, 2009, **25**, 8226-8234.
16. W. J. Zhang, M. K. S. Li, P. L. Yue and P. Gao, *Langmuir*, 2008, **24**, 2663-2670.
17. R. Z. Ma, Z. P. Liu, L. Li, N. Iyi and T. Sasaki, *J. Mater. Chem.*, 2006, **16**, 3809-3813.
18. M. Osada and T. Sasaki, *J. Mater. Chem.*, 2009, **19**, 2503-2511.
19. G. Abellan, E. Coronado, C. Marti-Gastaldo, E. Pinilla-Cienfuegos and A. Ribera, *J. Mater. Chem.*, 2010, **20**, 7451-7455.
20. S. Huang, H. D. Peng, W. W. Tjui, Z. Yang, H. Zhu, T. Tang and T. X. Liu, *J. Phys. Chem. B*, 2010, **114**, 16766-16772.
21. Q. L. Wu, A. Olafsen, O. B. Vistad, J. Roots and P. Norby, *J. Mater. Chem.*, 2005, **15**, 4695-4700.
22. R. Z. Ma, Z. P. Liu, K. Takada, N. Iyi, Y. Bando and T. Sasaki, *J. Am. Chem. Soc.*, 2007, **129**, 5257-5263.
23. L. Li, R. Z. Ma, N. Iyi, Y. Ebina, K. Takada and T. Sasaki, *Chem. Commun.*, 2006, 3125-3127.
24. L. Li, R. Z. Ma, Y. Ebina, N. Iyi and T. Sasaki, *Chem. Mater.*, 2005, **17**, 4386-4391.
25. D. C. Ford, Y. Xu and M. Mavrikakis, *Surf. Sci.*, 2005, **587**, 159-174.
26. D. Liu, S. Kyriakides, S. W. Case, J. J. Lesko, Y. X. Li and J. E. McGrath, *J. Polym. Sci. Polym. Phys.*, 2006, **44**, 1453-1465.
27. D. Bograchev, M. Gueguen, J. C. Grandidier and S. Martemianov, *Int. J. Hydrogen Energy*, 2008, **33**, 5703-5717.

1

**Table of Contents:**

2



3 A fuel cell with a 9 $\mu$ m thick proton exchange membrane bearing Pt-nanosheet catalysts  
4 delivered 200% more power density as compared with the fuel cell with commercial Nafion<sup>®</sup>  
5 112 membrane.